

Article

Preparation of Polymer Solution for Profile Control and Displacement Using Wastewater with High $\text{Ca}^{2+}/\text{Mg}^{2+}$ and Fe^{2+} Concentrations

Xuanran Li ¹, Anzhu Xu ¹, Mengqi Ma ^{2,*}, Shanglin Liu ¹, Jun Ni ¹ and Lun Zhao ¹¹ Research Institute of Petroleum Exploration and Development (RIPED), Beijing 100083, China² College of Petroleum Engineering, China University of Petroleum, Beijing 102249, China

* Correspondence: mengqi_maggie@163.com; Tel.: +86-136-9125-2916

Abstract: In the present study, we used Kalamkas, which is a typical Kazakhstani oilfield, which produces wastewater with high $\text{Ca}^{2+}/\text{Mg}^{2+}$ and Fe^{2+} concentrations, as a case study. We investigated a method for preparing Fe^{2+} polymer solutions without oxygen isolation under the conditions of salinity $>110 \times 10^3$ mg/L, $\text{Ca}^{2+}/\text{Mg}^{2+}$ concentration >7000 mg/L, and Fe^{2+} concentration >30 mg/L. Fe^{2+} -resistant groups were grafted onto the molecular chains of a hydrophobically associating polymer prepared using existing synthesis technology to overcome the decrease in apparent viscosity of the polymer solution due to the oxidation of Fe^{2+} during solution preparation. The experiments showed that PAM-IR with iron-resistant groups can be completely dissolved in the wastewater within 180 min, and can tolerate an NaCl concentration of up to 0.23×10^6 mg/L, a Ca^{2+} concentration of up to 10×10^3 mg/L, an Mg^{2+} concentration of up to 9×10^3 mg/L, and a Fe^{2+} concentration of up to 90 mg/L, with favorable thickening performance and resistances to NaCl, Ca^{2+} , Mg^{2+} , and Fe^{2+} . PAM-IR has good injection performance and can establish a high resistance factor (F_R) and residual resistance factor (F_{RR}) to increase the sweep efficiency. Therefore, it is potentially useful for enhancing oil recovery.



Citation: Li, X.; Xu, A.; Ma, M.; Liu, S.; Ni, J.; Zhao, L. Preparation of Polymer Solution for Profile Control and Displacement Using Wastewater with High $\text{Ca}^{2+}/\text{Mg}^{2+}$ and Fe^{2+} Concentrations. *Processes* **2023**, *11*, 325. <https://doi.org/10.3390/pr11020325>

Academic Editors: Linhua Pan, Yushi Zou, Jie Wang, Minghui Li, Wei Feng, Lufeng Zhang and Qingbang Meng

Received: 31 October 2022

Revised: 30 December 2022

Accepted: 13 January 2023

Published: 19 January 2023



Copyright: © 2023 by the authors. Licensee MDPI, Basel, Switzerland. This article is an open access article distributed under the terms and conditions of the Creative Commons Attribution (CC BY) license (<https://creativecommons.org/licenses/by/4.0/>).

Keywords: formation water with high salinity; Fe^{2+} -resistant polymer; apparent viscosity; resistance factor; microscopic state

1. Introduction

It is common to extract chemical reagents from oilfield wastewater produced during polymer flooding or in-depth profile control flooding. The strategy is environmentally friendly and economical. However, this method requires a high-performance chemical displacement agent, especially if the concentrations of $\text{Ca}^{2+}/\text{Mg}^{2+}$ and Fe^{2+} are high, which will seriously affect the performance of the chemical displacement agent [1–7].

The effect of polymer flooding varies considerably depending on the reservoir [1,8,9], and the water used for preparing the polymer solution. Wastewater contains inorganic salts, divalent and high-valence ions, sulfides, solid impurities, crude oil, and bacteria. When it is used directly to prepare a polymer solution, the viscosity of the generated flooding system is significantly reduced [2,8,9]. Previous studies [3–5,10–14] have indicated that cations affect the stability of a polymer solution in the order: $\text{Fe}^{2+} > \text{Fe}^{3+} > \text{Mg}^{2+}$ (Ca^{2+}) $> \text{Na}^+$ (K^+). When the polymer is diluted with wastewater containing Fe^{2+} at a concentration of 1700 mg/L, the viscosity of the polymer solution measured at 70 °C is less than 5 mPa·s, and the viscosity retention rate is less than 10%, both of which seriously impede the displacement effect. A water quality survey has shown that the Fe^{2+} concentration of the wastewater is greater than 0.5 mg/L. According to the laboratory results reported in the literature [3–6,10–15], the Fe^{2+} concentration of the injected water is the main factor that affects the viscosity of the polymer solution during in-depth profile control [9]. Therefore,

the polymer solution is often prepared directly using fresh water (e.g., at the Xinjiang oilfield in China), or prepared using fresh water that is then diluted with wastewater (e.g., at the Daqing oilfield in China) [11]. Many researchers have proposed adding chemicals (e.g., alcohols, thiourea, formaldehyde, or sodium borohydride) to the polymer to eliminate the influence of Fe^{2+} through reactions, wherein the molecular chain of the polymer is unaffected by the oxidation reactions of Fe^{2+} . This method can reduce the solid content of the polymer, but it significantly increases its cost. Other researchers have also mentioned the use of physical oxygen isolation methods (e.g., nitrogen production and oxygen isolation, and the improved design of fluid transfer systems) [16–18]. However, these methods also have poor economic benefits, and impose high demands on the injection equipment. Therefore, they are not conducive to long-term use. Moreover, the results from laboratory tests and from actual field application differ. The methods described above may require large amounts of clean water or involve the treatment of wastewater. The consumption of clean water resources and the cost of wastewater treatment both increase the input of oilfields and the risk of environmental pollution while reducing the overall economic benefits of polymer flooding. Therefore, only if the comprehensive effect of reducing wastewater treatment and increasing oil production can maximize the benefits to the oilfield, will they promote the application of the technology.

The Kalamkas oilfield in the North Uschut Basin of Kazakhstan is a stratified unintegrated reservoir with a gas cap and edge water. It is one of the high-aquifer sandstone reservoirs that are typical of Kazakhstan, and has an average reservoir thickness of 14 m, an average porosity of 0.27, and an average permeability of 441 millidarcy (mD). It has been developed for 42 years. Currently, most wells have a water cut of more than 95%, and the vertical production degree of the oilfield is only approximately 50%. Ineffective water injection is a serious problem, and production efficiency is low, which adversely affects recovery. The problem of ineffective water circulation during the development process needs to urgently be solved. In light of the experience gained through the development of medium–high-permeability sandstone oilfields throughout the world, the Kalamkas oilfield is believed to be suitable for in-depth profile control. However, the oilfield is developed by re-injecting the wastewater, which has a salinity of $>110 \times 10^3$ mg/L, a $\text{Ca}^{2+}/\text{Mg}^{2+}$ concentration of >7000 mg/L, an oil content of >70 mg/L, and, most importantly, a Fe^{2+} concentration of 30–70 mg/L. In addition, there is no water treatment system. These conditions are technically and economically far from the requirements for polymer solution preparation and injection; therefore, it is difficult to screen out economically feasible polymers, which makes the preparation of a flooding agent challenging [19]. Therefore, it is necessary to develop proper Fe^{2+} -resistant polymers to enhance oil recovery, lower costs, and improve economic performance at the Kalamkas oilfield.

The present paper describes the development of a new Fe^{2+} -resistant polymer for the preparation of a polymer solution using oilfield wastewater with a high Fe^{2+} concentration and high salinity. According to ShiraziM1 and other authors [20–26], a hydrophobically associating polymer solution is stable under conditions of high salinity and high temperature and, therefore, is useful as a flooding agent. During wastewater treatment, complex compounds are generally used to stabilize Fe^{2+} [27]. Dong and Lin et al. adopted oxygen isolation to mitigate the reduction in polymer viscosity due to Fe^{2+} oxidation [28]. Since 2014, a nitrogen blanketing system has been used to isolate air at the Kalamkas oilfield to eliminate the degradation of the polymer solution caused by Fe^{2+} oxidation [17]. Cao et al. and Xiong et al. have indicated that certain hydrophobically associating polymers can form three-dimensional network morphologies that improve thickening performance. They further divulged that such hydrophobically associating polymers are water-soluble and are formed by introducing a small amount (generally $< 2\%$) of an associating functional monomer into a polyacrylamide molecular chain. Polymers synthesized from various functional monomers have distinct molecular structures and functions. The hydrophobically associating polymers described have potential for use in polymer flooding, as viscosity modifiers for fracturing fluids, or for heat-resistant, salt-tolerant filtrate reducers for water-

based drilling fluids [29–33]. In the present study, we attempted to graft Fe^{2+} -resistant groups onto the molecular chain of a hydrophobically associating polymer to form a kind of 3D network that can trap Fe^{2+} while maintaining the viscosity of the polymer solution. This polymer ensures that the high viscosity and long-term stability of a solution prepared using oilfield sewage are retained.

2. Materials and Methods

2.1. Materials and Instruments

The chemicals used to prepare the experimental samples comprised: NaCl, CaCl_2 , $\text{MgCl}_2 \cdot 6\text{H}_2\text{O}$, and $(\text{NH}_4)_2\text{Fe}(\text{SO}_4)_2 \cdot 6\text{H}_2\text{O}$, which were all of analytical purity (i.e., >99%); acrylamide (AM), acrylic acid (AA), NaOH, ammonium persulfate ($(\text{NH}_4)_2\text{S}_2\text{O}_8$), sodium bisulfite (NaHSO_3), octadecyl dimethyl allyl ammonium chloride (DMAAC-18), and *N,N*-methylene bisacrylamide (MBA), which were all industrial products (with purities > 98%); hydrolyzed polyacrylamide (HPAM), with a molecular weight of 23×10^6 , a solid content of 90.0%, and a hydrolysis degree of 22.5%, which is commonly used for flooding in China's Daqing and Xinjiang oilfields, and was provided by Xinjiang Keli New Technology Development Co., Ltd. Karamay, China, and a hydrophobically associating water-soluble polymer (HAWP) comprising a Fe^{2+} -resistant polyacrylamide with a molecular weight of 12×10^6 , a solid content of 90.0%, and a hydrolysis degree of 20%.

Simulated brine, with a salinity of 116,700 mg/L, was prepared by adding 90.17 g of NaCl, 15.00 g of CaCl_2 , and 24.68 g of $\text{MgCl}_2 \cdot 6\text{H}_2\text{O}$ to 1 L of distilled water.

The wastewater sample from the Kalamkas oilfield was turbid, yellow, and oily, with a salinity of 124,991.1 mg/L, a density of 1.084 g/cm^3 , a pH of 6.67, a $\text{K}^+ + \text{Na}^+$ concentration of 40,427.1 mg/L, a Ca^{2+} concentration of 5611.2 mg/L, an Mg^{2+} concentration of 1702.4 mg/L, a Fe^{3+} concentration of 3.81 mg/L, a Fe^{2+} concentration of 33.46 mg/L, a Cl^- concentration of 77,103.75 mg/L, a HCO_3^{3-} concentration of 164.64 mg/L, a CO_2 concentration of 145.76 mg/L, and a total hardness of 420 mg/L. No SO_4^{2-} , CO_3^{2-} , or dissolved O_2 were found.

The core comprised of an epoxy resin cement (with approximate dimensions of $3.8 \text{ cm} \times 30 \text{ cm}$), with a N_2 -logging permeability of 390–410 mD, taken from the Kalamkas oilfield, where the average reservoir permeability is 400 mD.

The instruments comprised: a FD240-Binder convection oven; a ME2002 electronic balance (Mettler Toledo Instruments); an MCR302 advanced rheometer (Anton Paar); a scanning electron microscope (SEM); a VERTEX 70 Fourier-transform infrared spectroscopy (FTIR) spectrometer; a constant-temperature and constant-pressure displacement unit (Changzhou Yiyong, China); and a Fe-HX-10 quick iron-measuring tube (Beijing Huaxing, China). The other commonly available test devices comprised a heating mantle, Erlenmeyer flasks, and a cylinder containing 99.6% pure nitrogen.

2.2. Experimental Methods and Contents

In this study, the experiments on the preparation of polymer solution, the influence of metal ions on the viscosity of the polymer, the characteristic viscosity number, the molecular weight, and others were performed with the methods given in the Recommended Practices for Evaluation of Polymers Used in Enhanced Oil Recovery (SYT6576-2003), which is equivalent to API RP 63:1990. The experiments on resistance factor (F_R) and residual resistance factor (F_{RR}) were completed in accordance with the Technical Criteria of Polymer for Oil Displacement (SY/T5862-2020). Other experiments were conducted according to the literature [2,4,11–13,26,32]. The experiments are described as follows:

(1) Preparation of polymer solution

Simulated brine was used for preparing the polymer solution at normal temperature. We took a certain volume of simulated brine and stirred it with a stand blender at $(400 \pm 20) \text{ r/min}$. Then, we weighed the polymer with a mass required for preparing the solution with the designed polymer concentration and added it into the simulated brine being stirred. We further stirred (usually for 2–3 h) and observed the solution until the

particulate matters were completely dissolved, that is, until there was no “fisheye” in the solution and the insoluble particulate matters disappeared.

(2) Effect of Fe^{2+} on the viscosity of the polymer solution

We prepared a 1000 mg/L Fe^{2+} solution from $(\text{NH}_4)_2\text{Fe}(\text{SO}_4)_2 \cdot 6\text{H}_2\text{O}$ and added the simulated brine (116,700 mg/L) with Fe^{2+} concentrations of 1, 2, 5, 10, 20, 30, or 50 mg/L to form three 0.3% polymer solutions. We determined the solubility, and measured the apparent viscosity of each of the three polymer solutions at 3 h, then placed them in an incubator set to 40 °C. At 40 °C, and a shear rate of 10 s^{-1} , we measured the apparent viscosity changes at various time-points to determine the effect of Fe^{2+} on the various polymers and to assess the tolerance of these polymers with regard to Fe^{2+} .

(3) Measurement of Fe^{2+} concentration in the polymer solution

We measured the Fe^{2+} concentration before and after solution preparation using the quick iron-measuring tube to determine the changes in Fe^{2+} concentration, and to investigate the stability of Fe^{2+} in the polymer and assess the tolerance of the new polymer with regard to Fe^{2+} .

(4) Determination of the basic physical property parameters of the polymers

- (a) Characteristic viscosity and polymer molecular weight: The characteristic viscosity number $[\eta]$ of the polymer and weak gel was obtained by measurement of the Uhlerr viscosimeter, and the average molecular weight of the polymer and weak gel was calculated using the formula

$$[\eta] = K\bar{M}_v^a,$$

where K and a are empirical constants, $K = 6.31 \times 10^{-3}$, and $a = 0.8$ in the present paper.

- (b) Degree of hydrolysis: The degree of hydrolysis of the partially hydrolyzed polyacrylamide was determined by the method described in GB/T 12005.6-1989.

(5) Polymer characterization

The polymer microstructure was characterized by FTIR (VERTEX 70), and the infrared spectra of the synthesized samples was obtained. The microstructure of the polymer solution was characterized by SEM; hydrophobic association polymer (1500 mg/L) and Fe^{2+} -resistant polymer solutions were prepared with distilled water, and the microstates of the solutions were examined under a microscope.

- (6) Performance evaluation of the PAM-IR solution We prepared a 0.5% PAM-IR solution using simulated brine solutions with various concentrations of NaCl, Ca^{2+} , Mg^{2+} , and Fe^{2+} . We determined the state of the polymer in the solution at 3 h and measured its apparent viscosity to assess the resistance of the polymer solution to salinity and Fe^{2+} . The apparent viscosity was measured using the MCR302 rheometer at 40 °C and a shear rate of 10 s^{-1} . The experiments are performed on:

- (a) Salt sensitivity: various concentrations of NaCl were added to distilled water to form the simulated brines, which were then used to prepare polymer solutions.
- (b) Ca^{2+} influence: various concentrations of Ca^{2+} were added to a $100 \times 10^3 \text{ mg/L}$ NaCl aqueous solution to form simulated brines, which were then used to prepare polymer solutions.
- (c) Mg^{2+} influence: various concentrations of Mg^{2+} were added to a $100 \times 10^3 \text{ mg/L}$ NaCl aqueous solution to form simulated brines, which were then used to prepare polymer solutions.
- (d) Fe^{2+} influence: various concentrations of Fe^{2+} were added to a $100 \times 10^3 \text{ mg/L}$ NaCl aqueous solution to form simulated brines, which were then used to prepare polymer solutions.

(7) Verification experiment with wastewater

3.2. Results of Basic Physical Properties Determination

The synthesized samples were analyzed according to the experimental method described in Section 2.2 (3), and the results are shown in Table 1.

Table 1. Determination of the basic physical properties of the PAM-RI polymer.

Polymer	Characteristic Viscosity (dL/g)	Viscose Average Molecular Weight (10^6)	Degree of Hydrolysis (mol%)
PAM-RI	31.5	29.2	23.9

3.3. Characterization of the New Polymer

(1) FTIR analysis results

Figure 2 shows the infrared spectrum of the new polymer. The peak at $3500\text{--}3100\text{ cm}^{-1}$ is attributable to free NH_2 and associated NH_2 ; the peak at 2934 cm^{-1} is attributable to the antisymmetric stretching vibration of methylene; and the peak at 2333 cm^{-1} is attributable to the symmetric stretching vibration of methylene. The peak at 1681 cm^{-1} is attributable to the carbonyl group corresponding to amide ($\text{C}=\text{O}$ stretching vibration); the peak at 1560 cm^{-1} is attributable to the amide (N-H bending vibration); the peak at 1406 cm^{-1} is attributable to methylene deformation; and the peak at $770\text{--}550\text{ cm}^{-1}$ is attributable to the oscillation stretching vibration of N-H . All the profiles featured the characteristic absorption peaks of partially hydrolyzed polyacrylamide, proving the new polymer had been successfully prepared.

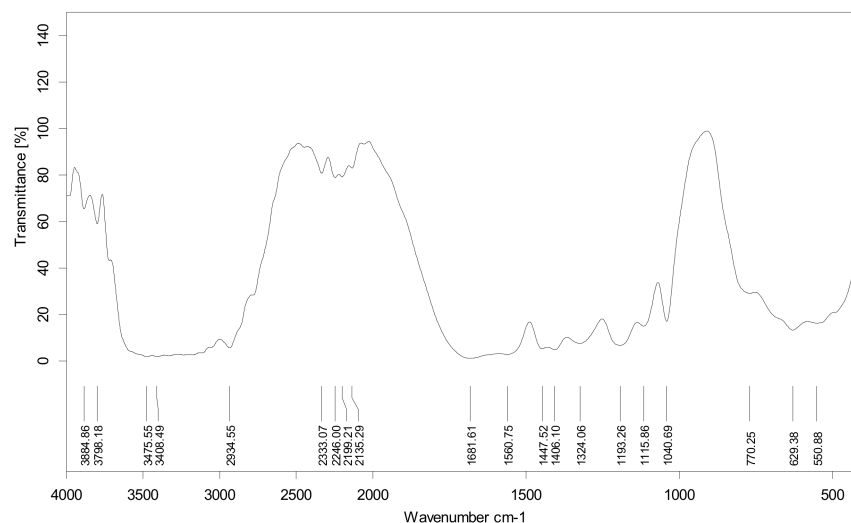


Figure 2. Infrared spectrum of the new polymer.

(2) SEM characterization results

As shown in Figure 3, we used SEM to investigate the 1500 mg/L HAWP and PAM-IR solutions prepared with distilled water for signs of the aggregation state and micro-morphology. HAWP exhibited a comb-shaped structure with functional groups, and a relatively regular three-dimensional network morphology, which is consistent with the findings described in the literature [7,32–34]. Similar to HAWP, PAM-IR presented a relatively regular three-dimensional network morphology, because the Fe^{2+} -resistant groups were grafted onto the branch chains of the hydrophobically associating polymers synthesized to avoid the viscosity reduction in the polymer solution while capturing the iron ions, so that the polymer solution prepared with oilfield wastewater has a high viscosity and a satisfactory long-term stability. Therefore, the morphology of PAM-IR, as shown in the SEM image, can allow the solution to be Fe^{2+} -resistant, and inherit the salt-resistant performance of HAWP.

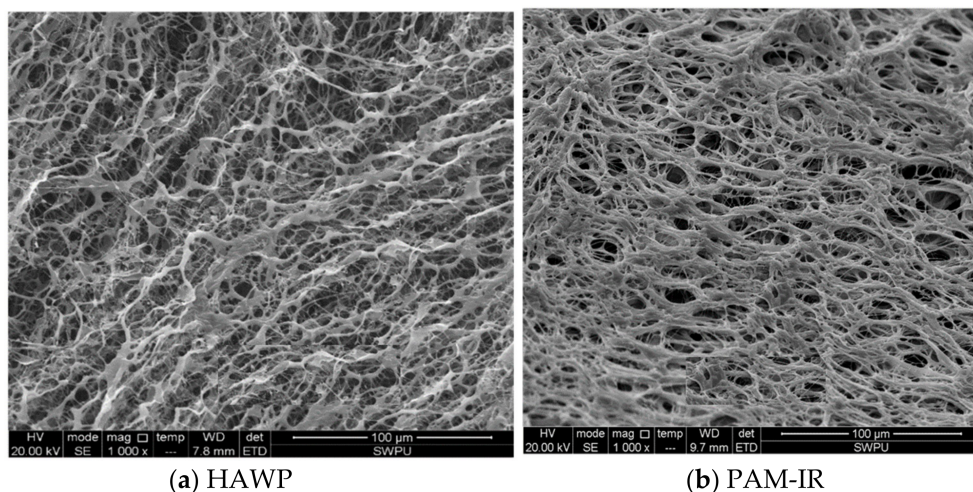


Figure 3. Microstructures of the polymer solutions. (a) Microstructure of HAWP; (b) Microstructure of PAM-IR.

3.4. Effect of Fe²⁺ on the Apparent Viscosity of the Polymer Solution

Three 0.3% polymer solutions were prepared using simulated Fe²⁺-containing brine solutions, and their solubilities at 3 h and apparent viscosities after dissolution were determined. The results are shown in Table 2 and Figure 4.

Table 2. Measured apparent viscosities of three polymers dissolved in simulated Fe²⁺-containing brine solutions.

Fe ²⁺ (mg/L)	Viscosity (mPa·s)								
	3 h			1 d			2 d		
	HPAM	HAWP	PAM-IR	HPAM	HAWP	PAM-IR	HPAM	HAWP	PAM-IR
0	28.0	60.7	47.5	27.7	60.3	47.5	28.0	60.5	47.2
1	26.5	55.2	47.2	26.5	58.2	47.2	25.3	55	47
2	24.2	45.3	47.3	24.2	46.5	47.3	20.5	45.2	46.5
5	13.8	40.5	47.2	13.5	20.5	46.2	12.5	11.2	43.2
10	3.5	20.3	46.5	11.3	3.2	45.5	3.2	4.5	42.1
20	2.5	15.2	46.3	10.3	2.1	45.3	2.1	3.5	41.5
30	2.5	11.2	45.3	5.2	2.3	44.1	2.2	3.5	41
50	2.3	8.5	42.5	3.2	2.2	42	1.5	2.5	40.8

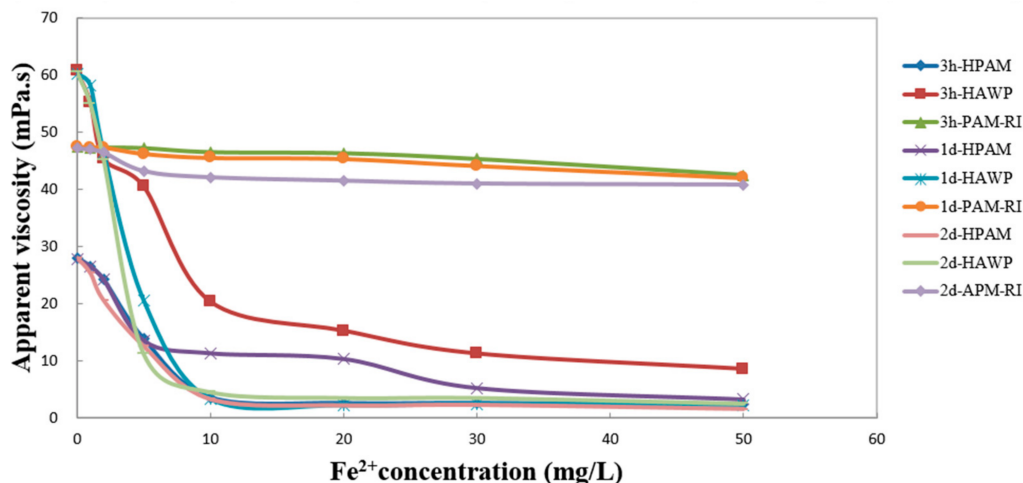


Figure 4. Fe²⁺ concentration versus apparent viscosity of the polymer solutions.

According to the results of the experiments involving dissolution at 3 h and the viscosity measurements, when the Fe^{2+} concentration of the simulated brine was 5 mg/L, the apparent viscosity of HPAM decreased to below 50%, the apparent viscosity of HAWP decreased to below 70%, and the apparent viscosity of PAM-IR remained almost unchanged, compared with that when the Fe^{2+} concentration of the simulated brine was 0. When the Fe^{2+} concentration of the simulated brine was 10 g/L, it was not possible to completely dissolve the HPAM or HAWP. When the Fe^{2+} concentration of the simulated brine was 50 mg/L, the apparent viscosity of HPAM was less than 10%, the apparent viscosity of HAWP was less than 20%, and the viscosity retention of PAM-IR was higher than 90%. The results are shown in Figure 5.

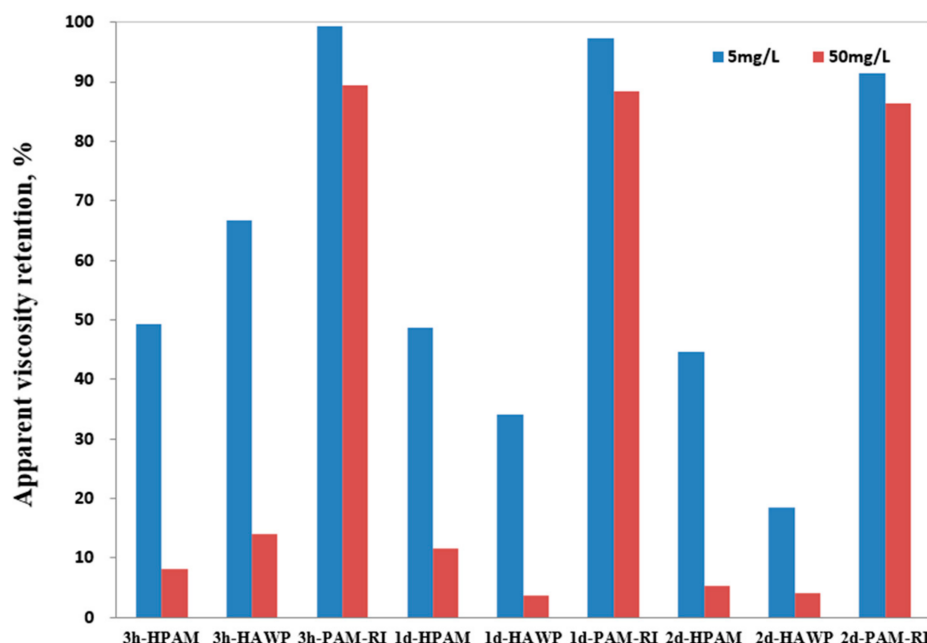


Figure 5. Apparent viscosity retention of polymer solutions with Fe^{2+} concentrations of 5 mg/L and 50 mg/L.

According to the results obtained after aging the polymer solutions at 40 °C after dissolution, the viscosity retention of PAM-IR remained above 90% over time, demonstrating favorable resistance to iron ions. In contrast, the apparent viscosity of HPAM decreased to less than 10%, which was close to the viscosity of the water sample. The apparent viscosity of HAWP decreased to less than 10%, also suggesting degradation.

3.5. Fe^{2+} Concentration of the Polymer Solution

The Fe^{2+} concentrations of the 0.3% polymer solutions were measured using the quick iron-measuring tube, and the color and Fe^{2+} concentration of the simulated water sample changed. The results are shown in Figures 6 and 7.

3.6. Evaluation of the Fe^{2+} -Resistant Polymers

We determined the state of the polymer at 3 h and measured the apparent viscosity of the 0.5% PAM-IR solution prepared using simulated brine solutions containing various concentrations of NaCl, Ca^{2+} , Mg^{2+} , and Fe^{2+} . As shown in Figures 8–12, PAM-IR can tolerate an NaCl concentration of up to 230×10^3 mg/L, a Ca^{2+} concentration of up to 10×10^3 mg/L, an Mg^{2+} concentration of up to 9×10^3 mg/L, and a Fe^{2+} concentration of up to 90 mg/L, respectively, demonstrating favorable thickening performance and resistance to NaCl, Ca^{2+} , Mg^{2+} , and Fe^{2+} .

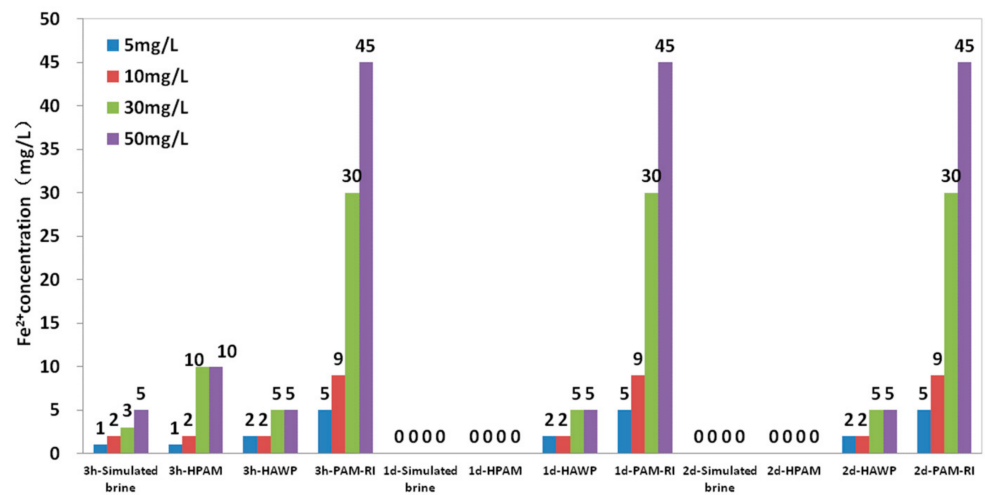


Figure 6. Measured Fe^{2+} concentrations of the polymer solutions.

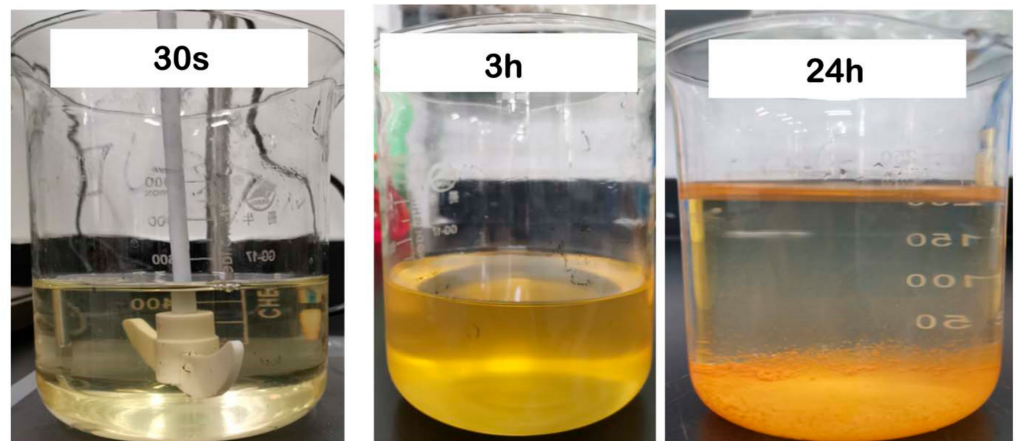


Figure 7. Changes in the simulated brine containing 50 mg/L Fe^{2+} .

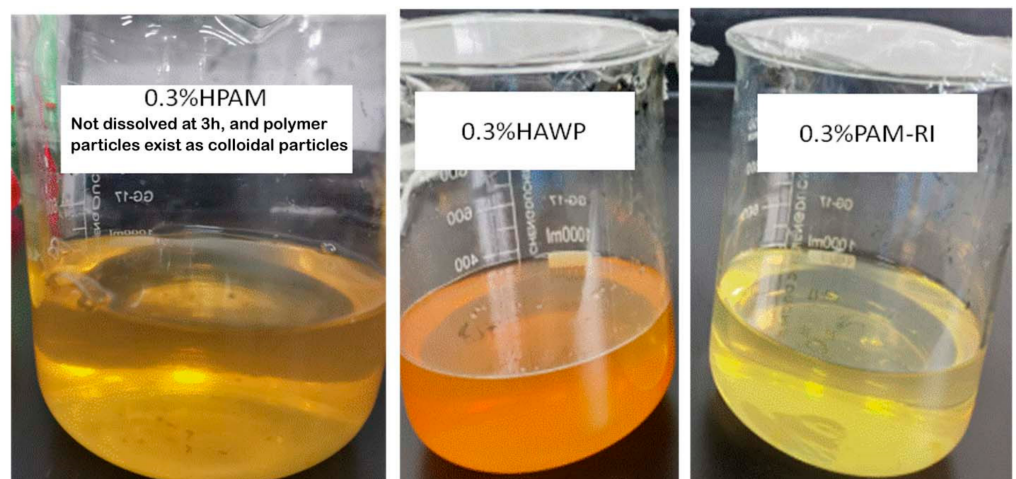


Figure 8. Changes in the three polymer solutions prepared with the simulated brine containing 50 mg/L Fe^{2+} at 3 h.

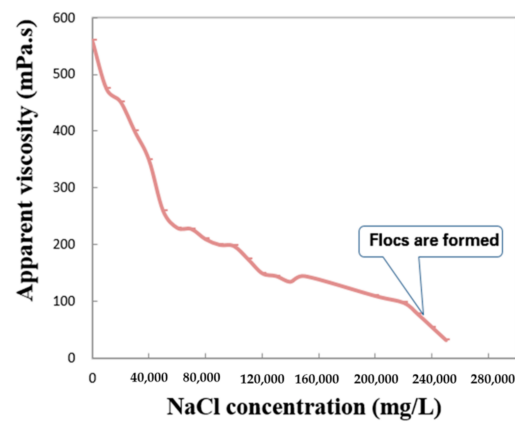


Figure 9. NaCl concentration versus apparent viscosity.

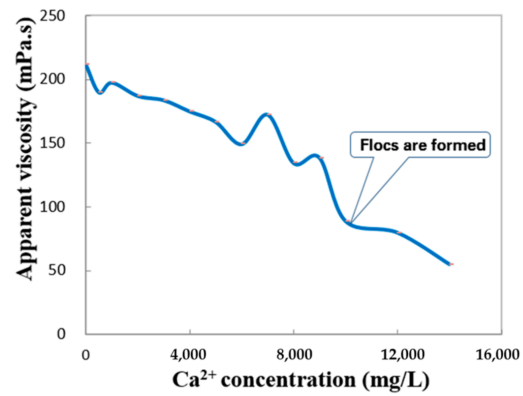


Figure 10. Ca²⁺ concentration versus apparent viscosity.

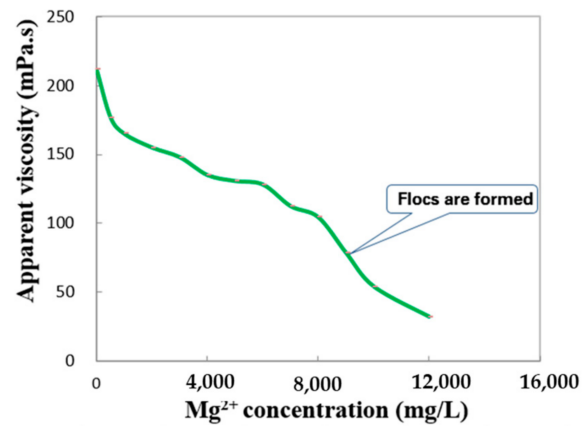


Figure 11. Mg²⁺ concentration versus apparent viscosity.

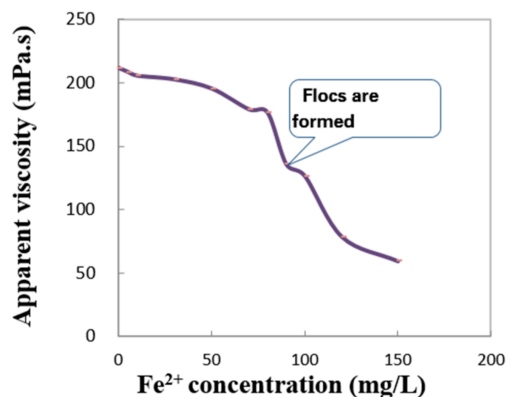


Figure 12. Fe²⁺ concentration versus apparent viscosity.

3.7. Verification with the Field Water Sample

The 0.5% polymer solutions were prepared using water collected from the Kalamkas oilfield and aerated water (the Fe²⁺ concentration was determined to be 0 after filtration). We determined the solubilities of the solutions and diluted them to polymer concentrations of 0.1–0.5%. As illustrated in Figures 13 and 14, the color of each polymer solution had not changed after 3 h, the polymer particles were completely dissolved, the apparent viscosity–polymer concentration curve was linear, and the viscosity reduction rate in the polymer solution prepared with raw water was 20% smaller than that of the polymer prepared with aerated water. Aeration completely removes the effect of iron ions on the viscosity of the polymer solution; however, high-salinity water loses calcium when it is aerated to remove iron ions. Thus, the concentrations of metal ions (e.g., Ca and Mg) in the aerated water were lower than those in the raw water, which produced different experimental results.

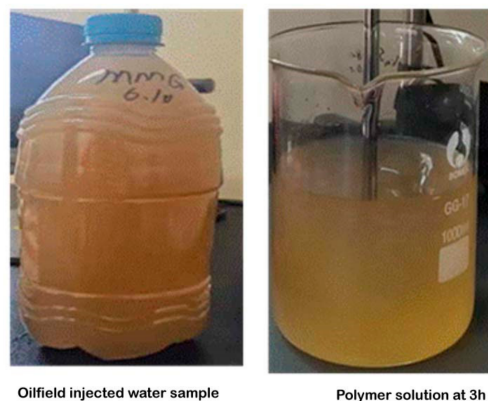


Figure 13. Injected water sample and polymer solution at 3 h.

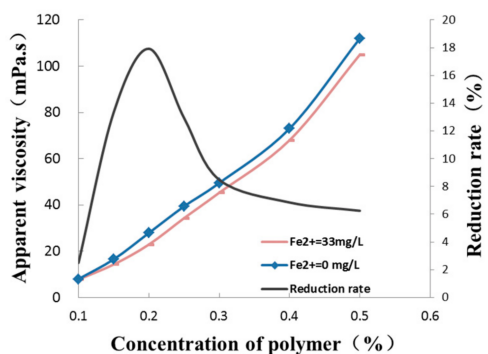


Figure 14. Apparent viscosity–polymer concentration curve.

3.8. Resistance Factor and Residual Resistance Factor Tests

The resistance factor and residual resistance factor are critical parameters for evaluating the concentration of a polymer solution in polymer flooding and are key indicators of the capacity of a polymer solution to improve the mobility ratio and reduce reservoir permeability [15,29,30]. In the present study, we determined the resistance factor (F_R) and residual resistance factor (F_{RR}) using a cement core with a permeability of approximately 400 mD after injecting polymer solutions of various concentrations at a rate of 1 mL/min at 40 °C. The test results are shown in Table 3 and Figure 15. As shown, the polymer solution was injected smoothly. During the injection process, the equilibrium pressure was reached, and no blockage formed. As the concentration of the injected polymer increased, F_R and F_{RR} increased. In actual applications, the polymer concentration can be selected depending on the oil viscosity and permeability of the reservoir.

Table 3. Test results showing the F_R and F_{RR} values of the polymer solutions.

Core	Gas Logging Permeability (mD)	Water Logging Permeability (mD)	Injected Polymer Concentration (%)	F_R	F_{RR}
1#	405.1	210.9	0.1	0.53	0.34
2#	410.5	226.5	0.2	3.39	1.57
3#	398.2	200.8	0.3	8.85	4.77
4#	402.8	210.5	0.4	19.29	11.64
5#	395.8	215.3	0.5	24.00	19.64

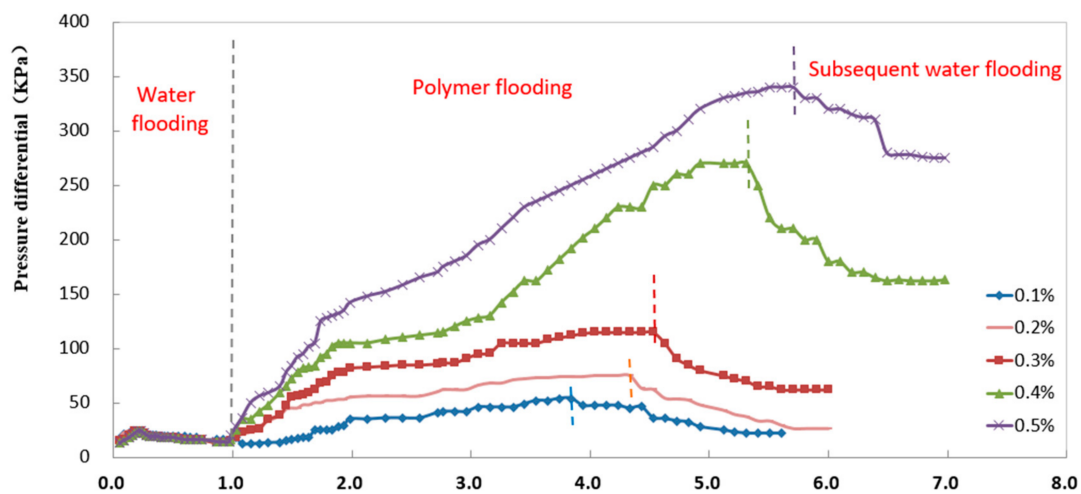


Figure 15. PV versus pressure differential.

4. Conclusions

- (1) The new polymer, PAW-IR, exhibits a relatively regular three-dimensional network morphology, and has a good solubility and a favorable thickening performance with regard to oilfield wastewater. It can be completely dissolved in oilfield wastewater within 180 min. It can tolerate an NaCl concentration of up to 23×10^4 mg/L, a Ca^{2+} concentration of up to 1×10^4 mg/L, an Mg^{2+} concentration of up to 0.9×10^4 mg/L, and a Fe^{2+} concentration of up to 90 mg/L, demonstrating favorable thickening performance and resistance to salt and Fe^{2+} .
- (2) PAM-IR is prepared by grafting the Fe^{2+} -resistant groups onto the branch chains of the traditional hydrophobically associating polymers synthesized to avoid the viscosity reduction in the polymer solution while capturing the iron ions. Compared with traditional physical methods (e.g., nitrogen production and oxygen isolation, and better design of fluid transfer) and chemical methods (e.g., the precipitation of Fe^{2+} by the addition of alcohol, formaldehyde, and sodium borohydride), the

- preparation of PAM-IR does not require additional investment and complex process design, which will improve the overall efficiency of polymer flooding in reservoirs with high concentrations of Fe^{2+} and $\text{Ca}^{2+}/\text{Mg}^{2+}$ in the formation water.
- (3) PAW-IR has a good injection performance and can establish high resistance factor and residual resistance factor, indicating a satisfactory plugging performance. It is promising for enhancing oil recovery by flooding with high-salinity and high- Fe^{2+} polymers.

Author Contributions: Conceptualization, X.L. and S.L.; methodology, X.L.; software, S.L.; validation, J.N., X.L. and M.M.; formal analysis, X.L. and J.N.; investigation, X.L.; resources, X.L.; data curation, M.M. and A.X.; writing—original draft preparation, X.L. and A.X.; writing—review and editing, M.M.; visualization, J.N.; supervision, L.Z.; project administration, J.N.; funding acquisition, L.Z. All authors have read and agreed to the published version of the manuscript.

Funding: This research was funded by the Major Science and Technology Projects of CNPC (grant number 2021DJ3201).

Institutional Review Board Statement: Not applicable.

Informed Consent Statement: Not applicable.

Data Availability Statement: Not applicable.

Conflicts of Interest: The authors declare no conflict of interest.

References

1. Alfazazi, U.; AlAmeri, W.; Hashmet, M.R. Screening of New HPAM Base Polymers for Applications in High Temperature and High Salinity Carbonate Reservoirs. In Proceedings of the Abu Dhabi International Petroleum Exhibition and Conference, Abu Dhabi, United Arab Emirates, 12–15 November 2018. SPE-192805-MS. [\[CrossRef\]](#)
2. Fan, J.; Wei, L.; Luo, W.L. Influencing Factors of the Viscosity Decrease on Polymer Sewage Solution. *Oilfield Chem.* **2011**, *28*, 251–253.
3. Chen, Y.; Li, D.; Song, H.; Song, Y. Research progress of the effect of metal cations on the viscosity of polyacrylamide solution. *J. Chem. Ind. Eng.* **2013**, *34*, 36–41.
4. Li, M.R.; Liu, Z.; Song, X.W.; Ma, B.D.; Zhang, W. Effect of metal ions on the viscosity of polyacrylamide solution and the mechanism of viscosity degradation. *J. Fuel Chem. Technol.* **2012**, *40*, 43–47.
5. YU, Y.; Sun, C.; Huang, J.; Yan, Y.; Li, X.; Xu, W.; Xing, L.; Wu, X.; Wang, J. Reconstruction Project of Iron Removal Process from Oilfield Produced Wastewater for Polymer Injection. *China Water Wastewater* **2012**, *10*, 66–69.
6. Wang, D.; Seright, R.S. Examination of literature on colloidal dispersion gels for oil recovery. *Pet. Sci.* **2021**, *18*, 1097–1114. [\[CrossRef\]](#)
7. Zaitoun, A.; Dupuis, G. Conformance control using SMG microgels: Laboratory evaluation and first field results. In Proceedings of the SPE Europe Featured at 79th EAGE Conference and Exhibition, Paris, France, 12–15 June 2017. [\[CrossRef\]](#)
8. Zhou, X.; Zhang, D. Analysis on Influence Factors of Formulating Polymer Solution with Sewage and Thickening Effect. *Contemp. Chem. Ind.* **2016**, *45*, 272–275.
9. Kang, W.L.; Meng, L.W.; Niu, J.G. Mechanism of the Effect of Salinity on HPAM Solution Viscosity. *Polym. Mater. Sci. Eng.* **2006**, *22*, 175–181.
10. Bin, C.; Xiaoyan, W.; Shanshan, W.; Shijia, C.; Qingquan, Z. Effect of Fe^{2+} on the apparent viscosity of polymer solution and controlling methods. *Chem. Eng. Oil Gas* **2014**, *43*, 168–173.
11. Wang, Z.; Wang, F.; Zong, H. Influence of iron ions on viscosity of polymer solution and its removal. *Ind. Water Wastewater* **2017**, *48*.
12. Ding, Y.; Zhang, J.; Ma, B.; Zhou, M.; Huang, M.; Li, M.; Hao, Q. Tackification Measures and Mechanism of Polymer Solution Prepared by Sewage. *Oilfield Chem.* **2013**, *32*, 123–127.
13. Yang, H.J.; Luo, P.Y. Factors for and Control of Polymer Degradation in Recycled Produced Water Solutions. *Oilfield Chem.* **2005**, *22*, 158–162.
14. Wang, Z.; Wang, Z. Discussion on Effective Reinjection Method of Produced Wastewater in Polymer Flooding. *Environ. Prot. Oil Gas Fields* **2018**, *22*, 40–42.
15. Yao, C.; Xu, X.; Wang, D.; Lei, G.; Xue, S.; Hou, J.; Steenhuis, T.S. Research and application of micron-size polyacrylamide elastic microspheres as a smart sweep improvement and profile modification agent. In Proceedings of the SPE Improved Oil Recovery Conference, Tulsa, OK, USA, 11–13 April 2016. [\[CrossRef\]](#)
16. Xing, E.; Tao, X.; Jin, L. Determination and Influence Factors of Resistance Coefficient and Residual Resistance Coefficient. *Liaoning Chem. Ind.* **2016**, *45*, 284–287.

17. Sagyndikov, M.; Salimgrayev, I.; Ogay, E.; KSeright, R.S.; Kudaibergnov, S.E. Assessing polyacrylamide solution chemical stability during a polymer flood in the Kalamkas field, Western Kazakhstan. *Bull. Univ. Kargnda-Chem.* **2022**, *105*, 99–112. [[CrossRef](#)]
18. Temizel, C.; Putra, D.; Zhang, M.; Moreno, R. Smart nanoparticles for conformance improvement in waterflooding. In Proceedings of the SPE Annual Caspian Technical Conference and Exhibition, Baku, Azerbaijan, 1–3 November 2017. [[CrossRef](#)]
19. Xiong, Z.; Deng, T.; Xu, H.; Jia, F.; Yu, X.; Ma, C. Performance evaluation on a hydrophobically associating polymer. *J. Guangdong Univ. Petrochem. Technol.* **2022**, *32*, 24–30.
20. Shirazi, M.; Kord, S.; Jamialahmadi, M.; Tamsilian, Y. Polymer Enhanced Oil Recovery Process: An Updated, Narrowed Review. *Acad. J. Polym. Sci.* **2018**, *1*, 555572. [[CrossRef](#)]
21. Mohsenatabar Firozjahi, A.; Zargar, G.; Kazemzadeh, E. An investigation into polymer flooding in high temperature and high salinity oil reservoir using acrylamide based cationic co-polymer: Experimental and numerical simulation. *Orig. Pap.-Prod. Eng.* **2019**, *9*, 1485–1494. [[CrossRef](#)]
22. Rellegadla, S.; Prajapat, G.; Agrawal, A. Polymers for enhanced oil recovery: Fundamentals and selection criteria. *Appl. Microbiol. Biotechnol.* **2017**, *101*, 4387–4402. [[CrossRef](#)]
23. Skauge, T.; Ormehaug, P.A.; Alsumaiti, A.; Masalmeh, S.; Skauge, A. Polymer Stability at Harsh Temperature and Salinity Conditions. In Proceedings of the SPE Conference at Oman Petroleum & Energy Show, Muscat, Oman, 21–23 March 2022.
24. Reichenbach-Klinke, R.; Langlotz, B.; Wenzke, B.; Spindler, C.; Brodt, G. Hydrophobic Associative Copolymer with Favorable Properties for the Application in Polymer Flooding. In Proceedings of the SPE International Symposium on Oilfield Chemistry, Woodlands, TX, USA, 11–13 April 2011.
25. Shi, L.; Chen, L.; Ye, Z.; Zhou, W.; Zhang, J.; Yang, J.; Jin, J. Effect of polymer solution structure on displacement efficiency. *Pet. Sci.* **2012**, *9*, 230–235. [[CrossRef](#)]
26. Zhi, L.I.U. Thickening Mechanism of Hydrophobically Associating Polyacrylamide and Polyacrylamide. *Acta Pet. Sin. (Pet. Process. Sect.)* **2012**, *28*, 1037–1042.
27. Wang, S.; Zhu, G.; Yu, Z.; Li, C.; Wang, D.; Cao, X. Ozonation Degradation of Fiber Water Catalyzed by Fe²⁺ Pyrophosphate Dodium Complex. *Spec. Petrochem.* **2020**, *37*, 15–21.
28. Dong, Z.X.; Lin, M.Q.; Xin, J.; Li, M.Y. Influence of dissolved oxygen content on oxidative stability of linked polymer solution. *Pet. Sci.* **2009**, *6*, 421–425. [[CrossRef](#)]
29. Zhang, H.; Wang, D.; Wang, L. Flow law of polymer solution in porous media and mechanism of improving oil displacement efficiency. *Daqing Pet. Geol. Dev.* **2002**, *21*, 57–61.
30. Xulong, C.A.O.; Yanfeng, J.I.; Yangwen, Z.H.U. Research advance and technology outlook of polymer flooding. *Reserv. Eval. Dev.* **2020**, *10*, 8–16.
31. Sagyndikov, M.; Mukhambetov, B.; Orynbasar, Y.; Nurbulatov, A.; Aidarbayev, S. Evaluation of Polymer Flooding Efficiency at brownfield development stage of giant Kalamkas oilfield, Western Kazakhstan. In Proceedings of the SPE Annual Caspian Technical, Conference and Exhibition, Astana, Kazakhstan, 31 October–2 November 2018. SPE-192555-MS.
32. Seright, R.S.; Wavrik, K.E.; Zhang, G.; AlSofi, A.M. Stability and Behavior in Carbonate Cores for New Enhanced-Oil-Recovery Polymers at Elevated Temperatures in Hard Saline Brines. *SPE Reserv. Eval. Eng.* **2003**, *24*, SPE-200324-PA. [[CrossRef](#)]
33. RSeright, R.S.; Skjevraak, I. Effect of Dissolved Iron and Oxygen on Stability of Hydrolyzed Polyacrylamide Polymers. *SPE J.* **2015**, *20*, 433–441. [[CrossRef](#)]
34. Jouenne, S. Polymer flooding in high temperature, high salinity conditions: Selection of polymer type and polymer chemistry, thermal stability. *J. Pet. Sci. Eng.* **2020**, *195*, 107545. [[CrossRef](#)]

Disclaimer/Publisher’s Note: The statements, opinions and data contained in all publications are solely those of the individual author(s) and contributor(s) and not of MDPI and/or the editor(s). MDPI and/or the editor(s) disclaim responsibility for any injury to people or property resulting from any ideas, methods, instructions or products referred to in the content.